Numerical simulation of flow around two 5:1 rectangular cylinders at a high Reynolds Number

Numerical simulation of flow around two 5:1 rectangular cylinders at a high Reynolds Number

G Yin[1,*], T Monaci[2] and M C Ong[1]

[1]Department of Mechanical and Structural Engineering and Materials Science, University of Stavanger, Stavanger, Norway
[2]CESI Engineering School, France

[*] Corresponding author: guang.yin@uis.no

Abstract. The unsteady flows around two stationary rectangular cylinders with a chord-to-thickness ratio of $B/D = 5$ at $Re_D = 2 \times 10^5$ (based on the free stream velocity and the width length D), are investigated using two-dimensional Unsteady Reynolds-Averaged Navier-Stokes equations with a standard $k - \omega$ SST turbulence model. The computational model is validated by carrying out simulation of the flow around a single rectangle and comparing the hydrodynamic quantities (time-averaged drag coefficient, root-mean-square of fluctuating lift coefficient) with the previous published data. The aim of the present study is to study the influence of the relative positions between the two rectangular cylinders on their hydrodynamic quantities and the surrounding flow fields.

1. Introduction

The developments of the offshore industries have increased the demanding for the investigation of the flow-structure interactions around marine structures. Flows around sharp-edged square and rectangular cylindrical structures are commonly seen in offshore and subsea engineering, such as submerged floating tunnels. These structures are often subject to high Reynolds number flows where strong currents are present. Since it is difficult to obtain the hydrodynamic quantities on the structures under the high Reynolds number flow conditions in experiments, Computational Fluid Dynamics (CFD) can serve as an efficient tool for the engineering design.

There have been extensively studies on the flows around rectangular cylinders with various aspect ratios. Early works includes the experimental measurements done by Okajima [12] on rectangular cylinders with aspect ratios from 1 to 4 in wind and water tunnels at Reynolds numbers ranging from 70 to 2×10^4. Nakamura & Yoshimura [11] used experiments to investigate the Strouhal number of the turbulent flow past rectangular cylinders with aspect ratio 0.2 to 5 at the Reynolds numbers (defined based on the height of the rectangle and the velocity of the inlet flow) of 5.5×10^3 to 1.4×10^5. Apart from experiments, numerical simulations have also been adopted to study the flow around rectangular cylinders with different aspect ratios. A benchmark case for the Benchmark on the Aerodynamics of a Rectangular 5:1 Cylinder (BARC) (Bartoli et al. [2]) was simulated using Large Eddy Simulation (LES) or Direct Numerical Simulation (DNS). The resulting force coefficients were in good agreement with the experimental data (Mannini et al. [8]). Mannini et al. [9] carried out two-dimensional (2D) Reynolds-averaged Navier-Stokes (RANS) simulations on the flow around a rectangular cylinder with an aspect ratio of 5:1 and compared the performance of different turbulence models.

Bruno et al. [3] performed 3D LES at $Re = 2 \times 10^5$ to study the fluctuating pressure field and it was found that the essential physics is 2D although the 3D flow features are observed. To the author's knowledge, most of the previous studies focused on the flows around a single rectangular cylinder. Only a few numerical studies have been conducted on the flow around two rectangular cylinders, which are frequently seen in many industries such as decks of two-tiered-bridges, offshore structures, heat exchangers, etc. The flow around two structures displays more complexity due to the interactions between shear layers, shedding vortices behind the structures. Therefore, it is important to study the effects of the arrangement of the two cylinders on the vortex dynamics behind the structures. Aboueian & Sohankar [1] carried out DNS of the flow over two square cylinders in staggered arrangement at a low Reynolds number of 150 for different gap spacing between cylinders to understand the flow structures. Lee et al. [7] used DNS to study the flow around a pair rectangular cylinders at a low Reynolds number of 100.

The goal of the present study is to extend the former studies to investigate the flow around two rectangular cylinders with different horizontal and vertical distances at a high Reynolds number, which has not been studied before. 2D RANS simulations are carried out. The $k-\omega$ SST model is used to resolve the turbulence stress. The paper is organized as follows. Section 2 gives a brief introduction to the mathematical formulation in the present study. The convergence study and the validation study are performed on the flow around a single rectangular cylinder to determine the grid and time-step resolution in Section 3. In Section 4, results of the flow around two rectangular cylinders are given. Finally, the conclusion is made in Section 5.

2. Mathematical Formulation

2.1. Flow Model

The unsteady Reynolds-averaged Navier-Stokes (URANS) equations for the conservation of mass and momentum are given by:

$$\frac{\partial u_i}{\partial x_i} = 0 \tag{1}$$

$$\frac{\partial u_i}{\partial t} + u_j \frac{\partial u_i}{\partial x_j} = -\frac{1}{\rho}\frac{\partial P}{\partial x_i} + \nu \frac{\partial^2 u_i}{\partial x_j^2} - \frac{\partial \overline{u_i{}' u_j{}'}}{\partial x_j} \tag{2}$$

where $i,j = 1,2$. Here x_1 and x_2 denote the streamwise (x) and cross-stream (y) directions respectively; u_1 and u_2 are the corresponding mean velocity components of the two direction (u, v); $\overline{u_i{}' u_j{}'}$ is the Reynolds stress component, where denotes the fluctuating part of the velocity; P is the pressure; ρ is the density of the fluid and t is the time.

The $k-\omega$ SST turbulence model (Menter [10]) is employed in the present study, which combines the $k-\omega$ and the $k-\varepsilon$ models. The original $k-\omega$ model of Wilcox [15] is used in the near-wall region and the standard $k-\varepsilon$ model of Jones & Launder [6] is adopted in the outer wake region and in the free shear layers. The detailed information of the $k-\omega$ SST turbulence model can be found in (Menter [10]; Tian et al. [14]; Jeong et al. [5]).

2.2. *Numerical setup*

The open source Computational Fluid Dynamics (CFD) code OpenFOAM (OpenFOAM v5) is used to carry out the simulations in the present study. The PISO (Pressure Implicit with Splitting of Operators) scheme (pisoFoam) is used. The spatial schemes for interpolation, gradient, Laplacian and divergence are linear, Gauss linear, Gauss linear corrected and Gauss linear schemes, respectively. All these schemes are in second order. The second order Crank-Nicholson scheme is employed for the time integration.

The computational domain is shown in Figure 1 for the single and the two rectangular cylinders. For the single rectangle cases, the origin of the coordinates is located at the centre of the rectangle. The

distances from the rectangle centre to the inlet and outlet boundaries are $10D$ and $30D$, respectively. The top and bottom boundaries are located at a distance of $10D$ to the centre of the rectangle. For the cases with two rectangles, the origin of the coordinates is set to be located at the midpoint of the connection line of the centres of the two rectangles. The distance from the origin to the inlet is $18D$ and the distance from the origin to the outlet is $54D$. The top boundary is located at a distance of $10D$ from the centre of Rectangle 1 (marked in Figure 1) and bottom boundary is located at a distance of $10D$ to the centre of Rectangle 2 (marked in Figure 2).

At the inlet boundary, the flow is set to be a uniform flow with $u_1 = U_\infty$, $u_2 = 0$. At the outlet boundary, the velocities are set as zero normal gradient and the pressure is set as zero. The top and bottom boundaries are set as symmetry planes. On the surface of the rectangles, no-slip boundary condition is applied for the velocities, i.e. $u_i = 0(i = 1,2)$and zero normal gradient condition is applied for the pressure. The standard near-wall condition for k and ω is applied on the surfaces of the rectangles.

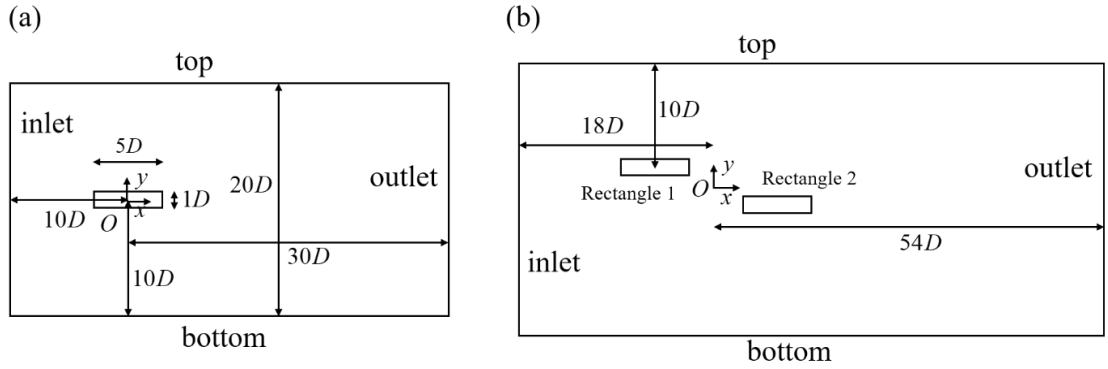

Figure 1. The computational domains for (a) the single rectangle case and (b) the two rectangles case.

3. Convergence studies and validation

The convergence studies are carried out for the single rectangle cases to determine the grid and time-step resolutions. The time-averaged drag coefficient ($\overline{C_d}$) and the root mean square of the lift coefficient (C_{lrms}) are considered, where the definitions of the two quantities are given as

$$\overline{C_d} = \frac{\overline{F_x}}{\frac{1}{2}\rho U_\infty^2 D} \tag{3}$$

$$C_l = \frac{F_y}{\frac{1}{2}\rho U_\infty^2 D} \tag{4}$$

$$C_{lrms} = \sqrt{\frac{1}{N}\sum_{i=1}^{N}\left(C_{l,i} - \overline{C_l}\right)^2} \tag{5}$$

where $\overline{F_x}$ is the time-averaged streamwise force acting on the rectangles per unit length and F_y is the cross-stream force acting on the rectangles per unit length, which are both computed from the integration of the pressure and viscous shear stress over the surface of the rectangles. N is the number of the sampling data.

Table 1 shows the results of the grid and time-step convergence studies of the single rectangle case. The differences of the numbers of the cells between cases are over 30%. The Courant numbers of all the simulations are kept below 0.4. It is shown that with the increasing number of cells, the maximum

relative difference of $\overline{C_d}$ is 0.38% (denoted as $\%\overline{C_d}$ in Table 1) and the maximum relative difference of C_{lrms} is around 5% (denoted as $\%C_{lrms}$ in Table 1). With the smaller time-step, the relative differences of $\overline{C_d}$ and C_{lrms} are also negligible. As a result, it can be concluded the mesh and time-step of Case 3 can provide sufficient grid resolution. It is noteworthy that since the wall function is applied on the surface of the rectangle, a criterion of $y^+ > 30$ (defined as $y^+ = u_\tau \Delta y/\nu$ where Δy is the distance of the centre of the first cells away from the wall and u_τ is the friction velocity on the surface of the rectangle) is achieved in every case. An example of the grids of Case 3 is shown in Figure 2.

Table 1. Results of grid and time-step convergence studies.

Case	Elements	y^+	$\Delta t U_\infty/D$	$\overline{C_d}$	$\%\overline{C_d}$	C_{lrms}	$\%C_{lrms}$
1	125825	31.66	0.001	1.1013	-	0.2643	-
2	190427	33.43	0.001	1.1041	0.2542	0.2737	3.5566
3	257187	32.92	0.001	1.1105	0.5797	0.2882	5.2978
4	257187	32.92	0.0008	1.1111	0.0540	0.2906	0.8259

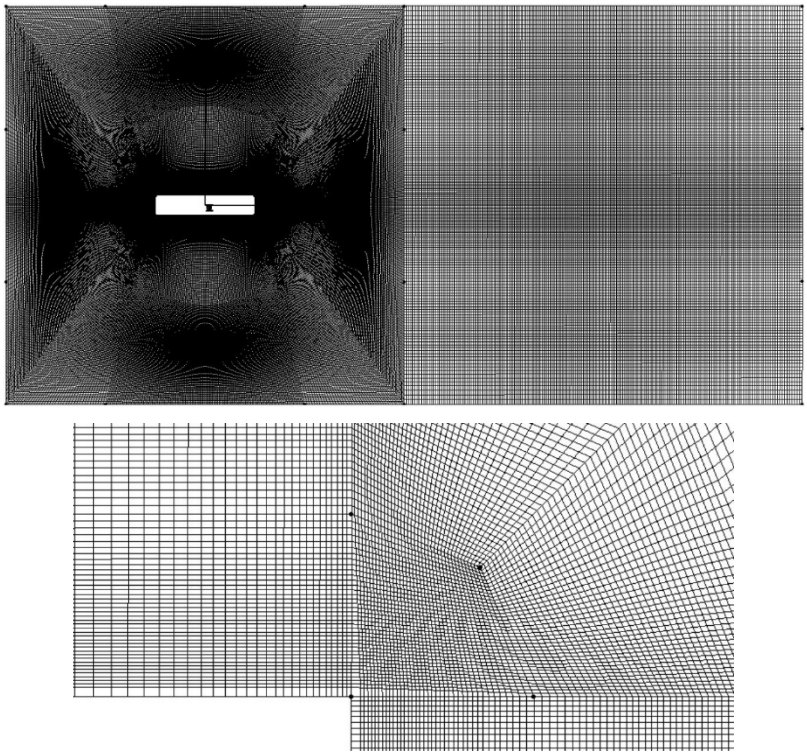

Figure 2. The computational mesh of case.

Validation studies are conducted by comparing the present results with the previous published data as shown in Table 2. It can be seen that $\overline{C_d}$ of the present study agrees well with the literatures while C_{lrms}, which is sensitive, is overpredicted compared with the numerical results at the same Reynolds number.

Table 2. Hydrodynamic quantities for rectangular cylinder with aspect ratio of 5:1.

Source / Author	Method	Re_D	$\overline{C_d}$	C_{lrms}
Present study	2D RANS $k-\omega$ SST	2×10^5	1.1105	0.2882
Dahl [4]	2D RANS $k-\varepsilon$	5×10^5	1.1008	0.2760
Bruno et al. [3]	3D LES	4×10^4	1.0500	0.7200
Mannini et al. [9]	3D DES	2.64×10^4	1.0290	0.4210
Schewe [13]	Exp.	2×10^4	1.0300	0.4000

4. Results and discussion

The grid resolution and time-step of the convergent results of Case 3 are used for the two rectangles cases. In the present study, four different combinations of (H, V) (H is the horizontal distance between the back face of Rectangle 1 and the front face of Rectangle 2 and V is the vertical distance between the bottom face of Rectangle 1 and the top face of Rectangle 2) are considered.

Time-averaged drag coefficients as well as the root-mean squares of the lift coefficients for the two rectangles (1 for Rectangle 1 and 2 for Rectangle 2) are displayed in Table 3. Figure 3 (a), (b) and Figure 4 (a), (b) show the time histories of the lift and drag coefficients of the two rectangles with different (H, V) in Table 3.

Table 3. Hydrodynamic quantities for two rectangular cylinders.

Cases	Elements	y^+(Rectangle 1/Rectangle 2)	$\overline{C_{d1}}$	C_{lrms1}	$\overline{C_{d2}}$	C_{lrms2}
$(H,V) = (0,1)D$	110000	35.12 / 35.18	1.391	0.032	1.388	0.030
$(H,V) = (0,3)D$	110000	31.90 / 32.73	1.244	0.121	1.248	0.129
$(H,V) = (3,1)D$	198000	30.38 / 32.59	1.042	0.111	1.196	0.529
$(H,V) = (6,1)D$	198000	30.50 / 31.61	1.047	0.100	1.142	0.389

For $(H,V) = (0,1)D$ and $(H,V) = (0,3)D$ with no horizontal distance between the two rectangles, $\overline{C_{d1}}$ and $\overline{C_{d2}}$ are almost the same. The sign of the lift coefficients of the two rectangles is opposite. This is due to the fact that the amplitudes of the low pressure regions above Rectangle 1 and below Rectangle 2 caused by the vortex are much stronger than the low pressure region between the two rectangles caused by high-velocity flow, as indicated in Figure 3 (c) and Figure 3 (d). With the increasing vertical distance between the two rectangles from $H = 1D$ to $H = 3D$, the root-mean-squares of the fluctuating lift coefficients of the two rectangles increase because of the increasing amplitude of the low pressure region between the two rectangles, as shown in Figure 3 (d). From the streamlines in Figure 3 (g) and Figure 3 (h), as the vertical distance increases, the small vortices below Rectangle 1 and above Rectangle 2 grow larger.

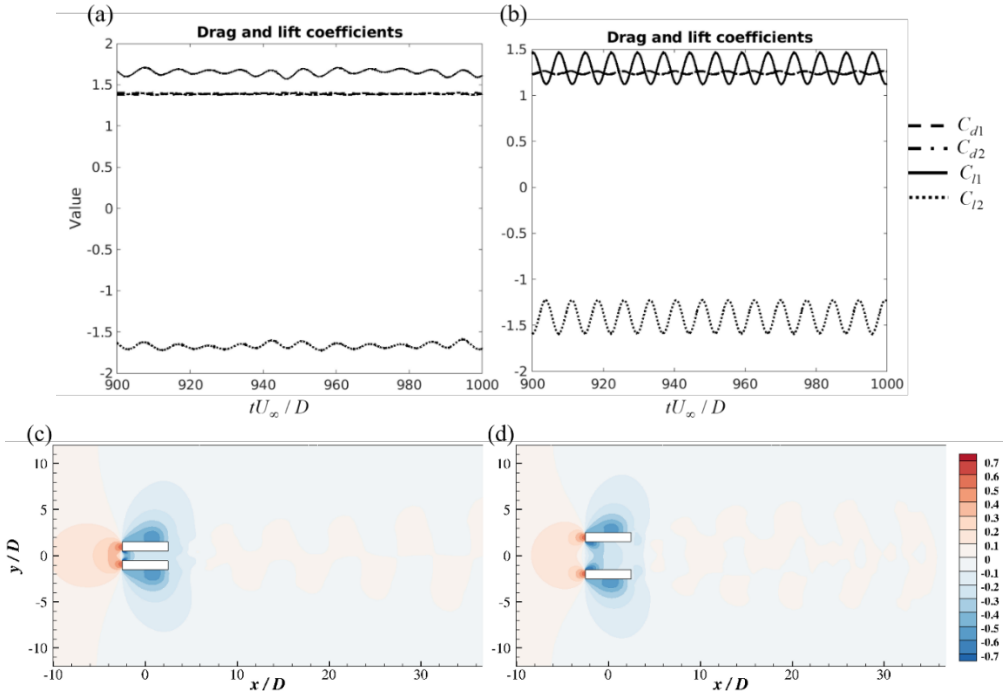

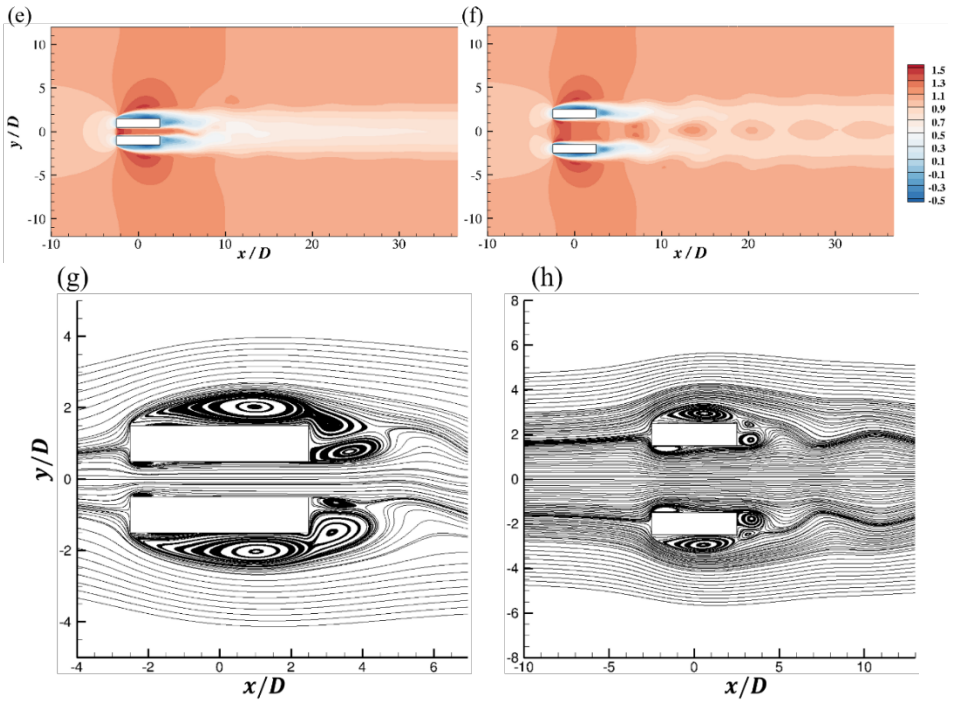

Figure 3. The Results for $(H,V) = (0,1)D$ (a), (c), (e), (g) and $(H,V) = (0,3)D$ (b), (d), (f), (h). (a),(b): time histories of C_{d1}, C_{l1} and C_{d2}, C_{l2}; (c),(d): instantaneous pressure $(2p/(\rho U_\infty^2))$ contours; (e),(f): instantaneous streamwise velocity (u/U_∞) contours; (g),(h): streamlines around the rectangles.

With a horizontal distance between the two rectangles, Rectangle 2 is influenced by the wake region behind Rectangle 1. As indicated in Figure 4 (a) and Figure 4 (b), the amplitudes of C_{lrms2} and $\overline{C_{d2}}$ are larger than those of Rectangle 1. With $(H,V) = (3,1)D$, the interaction between the surrounding flows of the two rectangles is strong, leading to an additional low-frequency oscillation modulating the high-frequency oscillation caused by the vortex shedding. This is more apparent for the lift coefficients than the drag coefficients as indicated in Figure 4(a). With the increasing H, this low-frequency oscillation disappears. This modulated periodic flow pattern has also been reported in Aboueian & Sohankar [1], where the flows around two staggered squares were studied. Instantaneous streamlines in Figure 4 (g) and Figure 4 (h) indicate that the vortices above Rectangle 2 is much larger than those in the cases with no horizontal distance where the vortices above Rectangle 2 are suppressed by the gap region between the two rectangles. This may be the contributor to the large amplitude of the lift coefficient of Rectangle 2.

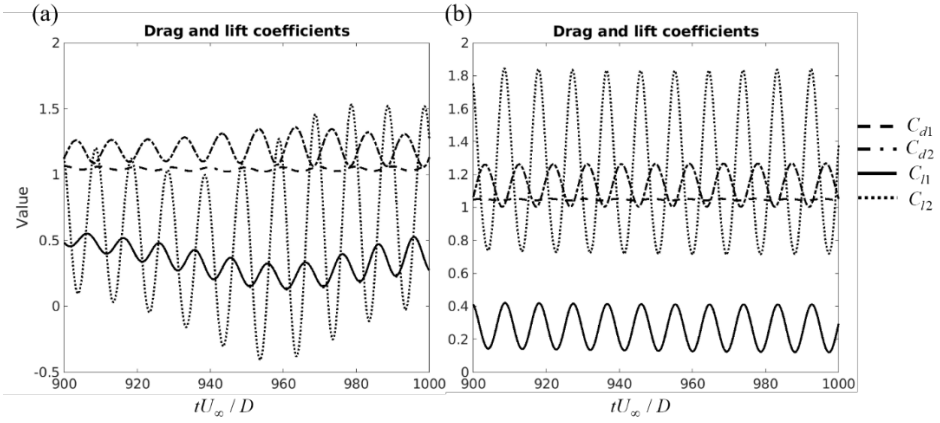

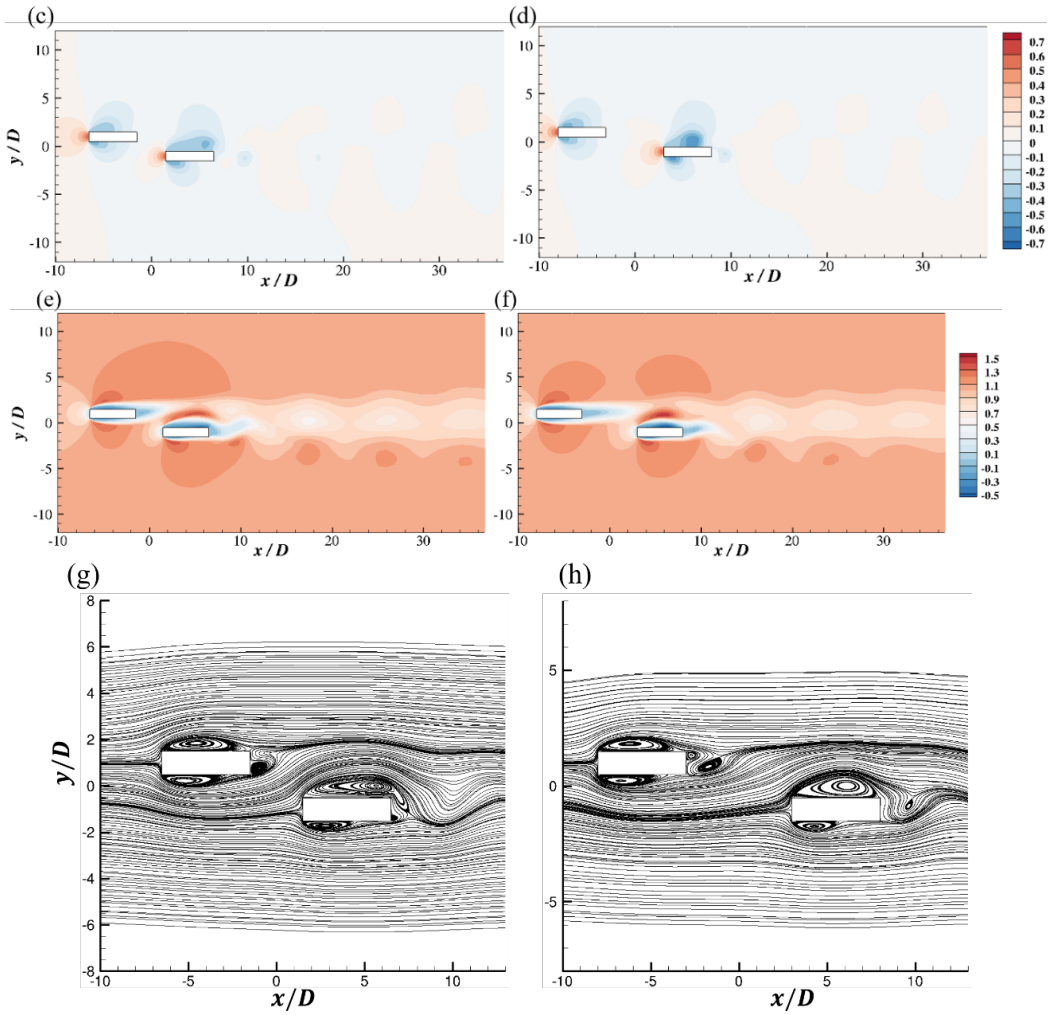

Figure 4. The Results for $(H,V) = (3,1)D$ (a), (c), (e), (g) and $(H,V) = (6,1)D$ (b), (d), (f), (h). (a),(b): time histories of C_{d1}, C_{l1} and C_{d2}, C_{l2}; (c),(d): instantaneous pressure $(2p/(\rho U_\infty^2))$ contours; (e),(f): instantaneous streamwise velocity (u/U_∞) contours; (g),(h): streamlines around the rectangles.

5. Conclusion

The flow around two rectangular cylinders with an aspect ratio of 5:1 has been simulated at a high Reynolds number of 2×10^5 using the 2D URANS combined with a standard $k-\omega$ SST and the wall function. The mesh and time-step convergence studies as well as the validation study have been carried out for the single rectangle case to prove the reliability of the present numerical model. The model is then applied to the two rectangle cases with different horizontal and vertical distances between them. It is found that with no horizontal distance, the drag coefficients of the two rectangles are almost the same. The lift coefficients of the two rectangles are opposite in sign with the same amplitude. As their vertical distance increases, the amplitude of the fluctuating lift coefficients of the two rectangles increases. With a horizontal distance, the lift coefficients display a modulated periodic flow pattern, which disappears with the increasing horizontal distance.

Acknowledgment

This study was supported with computational resources provided by the Norwegian Metacenter for Computational Science (NOTUR), under Project No: NN9372K.

References

[1] Aboueian J, and Sohankar A 2017. Identification of flow regimes around two staggered square cylinders by a numerical study, *Theor. Comput. Fluid Dyn.* **31**(3), 295-315.
[2] Bartoli G, Bruno L, Buresti G, Ricciardelli F, Salvetti M V and Zasso A 2008 BARC overview document. http://www.aniv-iawe.org/barc for further details (accessed 27/08/2019).
[3] Bruno L, Fransos D, Coste N and Bosco A 2010 3D flow around a rectangular cylinder: a computational study, *J. Wind Eng. Ind. Aerodyn.* **98**(6-7), 263-76.
[4] Dahl S M 2014 Unsteady RANS Simulation of Flow around Rectangular Cylinders with different Aspect Ratios at High Reynolds Number, Master's thesis, Institutt for marin teknikk, NTNU.
[5] Jeong W, Liu S, Jakobsen, J B and Ong M C 2019 Unsteady RANS Simulations of Flow around a Twin-Box Bridge Girder Cross Section, *Energies,* **12**(14) 2670.
[6] Jones W P and Launder B 1973 The calculation of low-Reynolds-number phenomena with a two-equation model of turbulence. *Int. J. Heat Mass Transfer*, **16**(6), 1119-30.
[7] Lee S J, Mun G S, Park Y G and Ha M Y 2019 A numerical study on fluid flow around two side-by-side rectangular cylinders with different arrangements, *J. Mech. Sci. Technol.* **33**(7), 3289-300.
[8] Mannini C, Šoda A and Schewe G 2010 Unsteady RANS modelling of flow past a rectangular cylinder: Investigation of Reynolds number effects, *Comput. Fluids,* **39**(9), 1609-24.
[9] Mannini C, Šoda A and Schewe G. 2011. Numerical investigation on the three-dimensional unsteady flow past a 5: 1 rectangular cylinder, *J. Wind Eng. Ind. Aerodyn.*, **99**(4), 469-82.
[10] Menter F R 1994 Two-equation eddy-viscosity turbulence models for engineering applications. *AIAA J.* **32**(8), 1598-1605.
[11] Nakamura Y and Yoshimura T 1982 Flutter and vortex excitation of rectangular prisms in pure torsion in smooth and turbulent flows, J. Sound Vib. **84**(3), 305-17.
[12] Okajima A 1982 Strouhal numbers of rectangular cylinders. *J. Fluid Mech.* **123**, 379-98.
[13] Schewe G 2013 Reynolds-number-effects in flow around a rectangular cylinder with aspect ratio 1: 5. J. Fluids Struct. **39** 15-26.
[14] Tian X, Ong M C, Yang J and Myrhaug D 2013 Unsteady RANS simulations of flow around rectangular cylinders with different aspect ratios, Ocean Eng. **58**, 208-16.
[15] Wilcox D C 1998 *Turbulence modeling for CFD* La Canada, CA: DCW industries.